HHS Public Access

Author manuscript

Chem Commun (Camb). Author manuscript; available in PMC 2018 August 11.

Published in final edited form as:

Chem Commun (Camb). 2017 August 11; 53(62): 8657–8659. doi:10.1039/c7cc04402j.

Radiofluorination of a NHC–PF_5 adduct: toward new probes for ^{18}F PET imaging†

Boris Vabre[‡,a], **Kantapat Chansaenpak**[‡,b,c], **Mengzhe Wang**[b], **Hui Wang**[b], **Zibo Li**[iD,§,b], and **François P. Gabbaï**[iD,§,a]

[a]Department of Chemistry, Texas A&M University, College Station, Texas 77843, USA [b]Department of Radiology, Biomedical Research Imaging Center, University of North Carolina, Chapel Hill 27599, USA [c]National Nanotechnology Center (NANOTEC), National Science and Technology Development Agency (NSTDA), 111 Thailand Science Park, Pathum Thani, 12120, Thailand

Abstract

The radiofluorination of N-heterocyclic carbene (NHC) phosphorus(V) fluoride adducts has been investigated. The results show that the IMe-PF_5 derivative (IMe = 1,3-dimethylimidazol-2-ylidene) undergoes a Lewis acid promoted ^{18}F–^{19}F isotopic exchange. The resulting radiofluorinated probe is remarkably resistant to hydrolysis both *in vitro* as well as *in vivo*.

A growing area of radiochemistry is concerned with the discovery of radiolabeled prosthetic groups which, once appended to tissue- or disease-specific biomolecules, provide a modular access to novel positron emission tomography (PET) imaging agents.[1] To date, most prosthetic groups contain a group 13 element[2–15] or a group 14 element[16–19] which serves as a binding site for the fluoride anion. Undoubtedly, boron-based prosthetic groups pioneered by Perrin are the most developed ones. The most versatile example of such a prosthetic group is the zwitterionic ammonium trifluoroborate (**I**) which can be incorporated in a wide range of peptide based radiotracers (Chart 1).[20–25] In parallel to these advances, our interinstitutional team introduced zwitterionic phosphoniumtrifluoroborates (**II**)[26,27] and NHC-BF_3 adducts (**III**) which, like **I**, can be conjugated to biomolecules.[27,28] Following up on these results, we were attracted to the fluorophilic properties of phosphorus(V) compounds.[29–31] Indeed, based on computed gas phase fluoride ion affinity data (346 kJ mol^{-1} for BF_3 and 380 kJ mol^{-1} for PF_5), which show that P(V) fluorides[31] may be more Lewis acidic than boron (**III**) derivatives, it occurred to us that phosphorus analogs of **III** might be ideally suited for application in PET.

†Electronic supplementary information (ESI) available: Experimental, characterization and imaging data. CCDC 1504579 and 1504580. For ESI and crystallographic data in CIF or other electronic format see DOI: 10.1039/c7cc04402j

Correspondence to: Zibo Li; François P. Gabbaï.

‡Contributed equally to the work.

§Jointly conceived the study.

Zibo Li http://www.orcid.org/0000-0002-5095-3761

François P. Gabbaï http://www.orcid.org/0000-0003-4788-2998

To explore this idea and expand on the limited chemistry of radiofluorinated phosphorus compounds,[32,33] we decided to investigate the radiofluorination of the N-heterocyclic carbene (NHC) phosphorus(V) fluoride derivatives **1** and **2**. Compound **1** was synthesized as described in the literature. To access compound **2**, we first synthesized and structurally characterized the potassium salt of the known anion $[PF_5Ph]^-$[34] *via* the "one pot" oxidation of $PPhCl_2$ using bromine in the presence of KF (Scheme 1 and Fig. S7, ESI†). This salt, whose ^{19}F and ^{31}P NMR spectra are consistent with those of other $[PF_5Ph]^-$ salts reported previously,[34] was successfully converted into the target compound **2** in 68% yield by the addition of *n*-BuLi at −78 °C to a mixture of imidazolium salt and $K[PF_5Ph]$ (Scheme 1). The ^{19}F NMR analysis of the crude mixture at room temperature after *n*-BuLi addition shows a doublet (J_{PF} = 849 Hz) for **2** at −43.9 ppm and a *cis* product with an approximate ratio of ~1:1 (Scheme 1). The *cis* adduct is characterized by three ^{19}F resonances with a relative integration of 2:1:1, respectively. These resonances include a doublet of virtual triplets at −57.6 ppm (J_{PF} = 783 Hz, J_{FF} = 40 Hz) and two doublets of doublets of triplets at −43.2 ppm (J_{PF} = 699 Hz, J_{FF} = 49 Hz, $J_{FF'}$ = 40 Hz) and −61.0 ppm (J_{PF} = 838 Hz, J_{FF} = 49 Hz, $J_{FF'}$ = 40 Hz). Heating this mixture at 66 °C for 26 h shows isomerisation of the *cis* product into the *trans* product **2** (Fig. S5 and S6, ESI†). Compound **2** is further characterized by a ^{31}P NMR resonance at 141.1 ppm split into a quintet (J_{PF} = 849 Hz). The ^{1}H NMR spectrum shows a characteristic singlet for the methyl substituents while the ^{13}C NMR spectrum shows two doublets of quintets at 150.0 ppm (J_{CF} = 43 Hz, J_{CP} = 297 Hz) and 159.8 ppm (J_{CF} = 71 Hz, J_{CP} = 334 Hz) corresponding to the phenyl *ipso*-carbon and carbene carbon, respectively. These assignments align with those reported for other NHC-PF_4Ph derivatives.[35] The structure of **2** has been confirmed by X-ray diffraction, which shows that the carbene–phosphorus C(1)–P(1) bond (1.898(2) Å) is only slightly longer than the C(6)–P(1) bond (1.839(2)) involving the phenyl group (Fig. 1).

The hydrolytic stability study of **1** and **2** was evaluated using a previously published method.[36] The compounds were dissolved in D_2O–CD_3CN (8/2 vol) at pH 7.5 ([phosphate buffer] = 500 mM) and the hydrolysis reaction was monitored by ^{19}F NMR spectroscopy. While the salt $K[PF_5Ph]$ shows a complete hydrolysis in less than 5 min, both carbene adducts **1** and **2** are highly water stable. Compound **2** undergoes a slow hydrolysis releasing free fluoride with a pseudo-first order rate constant (k_{obs}) of 2.3×10^{-5} min^{-1} (Fig. S8 and Table S3, ESI†). Surprisingly, we did not observe any free fluoride signal for **1** after five days, indicating that **1** can be considered as "eternal" (Fig. 2). It is more stable than the NHC-BF_3 analogue which shows a hydrolytic rate constant (k_{obs}) of 1.2×10^{-6} min^{-1} under the same conditions.[28]

Next, we investigated the radiofluorination of these compounds (Scheme 2). Compound **1** could be successfully radiolabeled *via* ^{18}F–^{19}F isotopic exchange using $SnCl_4$ as a promoter, a method that we pioneered in the preparation of [^{18}F]-BODIPY dyes.[37] In this experiment, compound **1** was mixed with 5 equiv. of $SnCl_4$ in MeCN and combined with a solution of [^{18}F]-TBAF in the same solvent (Table 1). The reaction mixture was then shaken for 10 min at different temperatures. After being quenched by the addition of water, the radiolabeled compound ([^{18}F]-**1**) was loaded on a Sep-Pak cartridge (Sep-Pak Plus *t*C18). Then, the excess tin reagent and by-products were removed using water. [^{18}F]-**1** was eluted off the

cartridge with MeCN. A portion of the resulting MeCN solution was subjected to HPLC analysis. The identity of [^{18}F]-**1** was confirmed by the comparison of its elution time with that of its non-radioactive analog **1** (Fig. 3).

As illustrated in Table 1, the radiochemical yields (RCY) of [^{18}F]-**1**, calculated based on the radio-activity of the isolated product and the starting radio-activity, are quite low (4–6% decay corrected RCY). These low yields originate from the stability of the P–F bonds which impedes the ^{18}F–^{19}F isotopic exchange process. We found that increasing the reaction temperature leads to higher radiochemical yields (entries 1–3). However, when a high reaction temperature (100 °C) was employed, [^{18}F]-**1** was not detected by either of the two HPLC modalities (radio and UV), indicating precursor decomposition (Fig. S9). Similar issues were encountered in the radiofluorination of **2**, for which all efforts proved unsuccessful including those involving different types of activators such as $SnCl_2$, $SnCl_4$, TMSOTf, HCl, and KHF_2.

The stability of [^{18}F]-**1** was first investigated in phosphate buffer solution (0.01 M, pH 7). [^{18}F]-**1** displayed >98% radiochemical purity even after an incubation time of 3 hours. This result suggested that [^{18}F]-**1** might be extremely stable under physiological conditions. The stability of [^{18}F]-**1** was further evaluated in a murine model. The probe [^{18}F]-**1** (0.1 mCi) was injected into female nude mice and static microPET scans were obtained at 3 hours after the injection. As shown in Fig. 4, the microPET/CT images showed an obvious localization in the bladder indicating that [^{18}F]-**1** was cleared through the urinary track. More importantly, no bone uptake was observed suggesting that the [^{18}F]-fluoride release was insignificant even 3 hours post-injection.

In conclusion, we report an organophosphorus [^{18}F]-radiotracer based on a N-heterocyclic carbene. Owing to Coulombic effects between the imidazolium and phosphate moieties, this probe is remarkably resistant to hydrolysis. It can nevertheless be radiolabeled by isotopic exchange when $SnCl_4$ is used as an acidic promoter and can be imaged using PET for as long as three hours post-injection. We are now exploring ways to functionalize this adduct such that it can be used as a prosthetic group for targeted tissue and disease imaging.

Supplementary Material

Refer to Web version on PubMed Central for supplementary material.

Acknowledgments

This work was supported by the Cancer Prevention Research Institute of Texas (RP130604), Texas A&M University (Arthur E. Martell Chair of Chemistry), the National Cancer Institute (P30-CA016086-35-37), and the Biomedical Research Imaging Center, University of North Carolina at Chapel Hill.

Notes and references

1. Miller PW, Long NJ, Vilar R, Gee AD. Angew. Chem., Int. Ed. 2008; 47:8998–9033.
2. Perrin DM. Acc. Chem. Res. 2016; 49:1333–1343. [PubMed: 27054808]
3. Chansaenpak K, Vabre B, Gabbai FP. Chem. Soc. Rev. 2016; 45:954–971. [PubMed: 26548467]

4. Liu ZB, Li Y, Lozada J, Schaffer P, Adam MJ, Ruth TJ, Perrin DM. Angew. Chem., Int. Ed. 2013; 52:2303–2307.
5. Liu Z, Hundal-Jabal N, Wong M, Yapp D, Lin KS, Benard F, Perrin DM. MedChemComm. 2014; 5:171–179.
6. Li Y, Ting R, Harwig CW, auf dKU, Bellac CL, Lange PF, Inkster JAH, Schaffer P, Adam MJ, Ruth TJ, Overall CM, Perrin DM. MedChemComm. 2011; 2:942–949.
7. Keller UAD, Bellac CL, Li Y, Lou YM, Lange PF, Ting R, Harwig C, Kappelhoff R, Dedhar S, Adam MJ, Ruth TJ, Benard F, Perrin DM, Overall CM. Cancer Res. 2010; 70:7562–7569. [PubMed: 20729277]
8. Ting R, Harwig C, auf dem Keller U, McCormick S, Austin P, Overall CM, Adam MJ, Ruth TJ, Perrin DM. J. Am. Chem. Soc. 2008; 130:12045–12055. [PubMed: 18700764]
9. Ting R, Adam MJ, Ruth TJ, Perrin DM. J. Am. Chem. Soc. 2005; 127:13094–13095. [PubMed: 16173707]
10. McBride WJ, Goldenberg DM, Sharkey RM. J. Nucl. Med. 2014; 55:1043.
11. McBride WJ, D'Souza CA, Sharkey RM, Goldenberg DM. Appl. Radiat. Isot. 2012; 70:200–204. [PubMed: 21890371]
12. McBride WJ, Sharkey RM, Karacay H, D'Souza CA, Rossi EA, Laverman P, Chang C-H, Boerman OC, Goldenberg DM. J. Nucl. Med. 2009; 50:991–998. [PubMed: 19443594]
13. Bhalla R, Levason W, Luthra SK, McRobbie G, Sanderson G, Reid G. Chem. – Eur. J. 2015; 21:4688–4694. [PubMed: 25652736]
14. Bhalla R, Darby C, Levason W, Luthra SK, McRobbie G, Reid G, Sanderson G, Zhang W. Chem. Sci. 2014; 5:381–391.
15. Khoshnevisan A, Jauregui-Osoro M, Shaw K, Torres JB, Young JD, Ramakrishnan NK, Jackson A, Smith GE, Gee AD, Blower PJ. EJNMMI Res. 2016; 6:34. [PubMed: 27103614]
16. Bernard-Gauthier V, Bailey JJ, Liu Z, Wängler B, Wängler C, Jurkschat K, Perrin DM, Schirrmacher R. Bioconjugate Chem. 2016; 27:267–279.
17. Bernard-Gauthier V, Bailey JJ, Liu Z, Wängler B, Wängler C, Jurkschat K, Perrin DM, Schirrmacher R. Bioconjugate Chem. 2016; 27:267–279.
18. Schirrmacher E, Wängler B, Cypryk M, Bradtmöller G, Schäfer M, Eisenhut M, Jurkschat K, Schirrmacher R. Bioconjugate Chem. 2007; 18:2085–2089.
19. Schirrmacher R, Bradtmöller G, Schirrmacher E, Thews O, Tillmanns J, Siessmeier T, Buchholz HG, Bartenstein P, Wängler B, Niemeyer CM, Jurkschat K. Angew. Chem., Int. Ed. 2006; 45:6047–6050.
20. Pourghiasian M, Liu Z, Pan J, Zhang Z, Colpo N, Lin K-S, Perrin DM, Bénard F. Bioorg. Med. Chem. 2015; 23:1500–1506. [PubMed: 25757604]
21. Liu Z, Amouroux G, Zhang Z, Pan J, Hundal-Jabal N, Colpo N, Lau J, Perrin DM, Bénard F, Lin K-S. Mol. Pharmaceutics. 2015; 12:974–982.
22. Liu Z, Lin K-S, Benard F, Pourghiasian M, Kiesewetter DO, Perrin DM, Chen X. Nat. Protoc. 2015; 10:1423–1432. [PubMed: 26313478]
23. Liu ZB, Pourghiasian M, Radtke MA, Lau J, Pan JH, Dias GM, Yapp D, Lin KS, Benard F, Perrin DM. Angew. Chem., Int. Ed. 2014; 53:11876–11880.
24. Liu ZB, Radtke MA, Wong MQ, Lin KS, Yapp DT, Perrin DM. Bioconjugate Chem. 2014; 25:1951–1962.
25. Liu Z, Perrin DM, Pourghiasian M, Benard F, Pan J, Lin K-S. J. Nucl. Med. 2014; 55:1499–1505. [PubMed: 24970911]
26. Li Z, Chansaenpak K, Liu S, Wade CR, Zhao H, Conti PS, Gabbaï FP. MedChemComm. 2012; 3:1305–1308.
27. Chansaenpak K, Wang M, Liu S, Wu Z, Yuan H, Conti PS, Li Z, Gabbai FP. RSC Adv. 2016; 6:23126–23133.
28. Chansaenpak K, Wang M, Wu Z, Zaman R, Li Z, Gabbai FP. Chem. Commun. 2015; 51:12439–12442.
29. Hudnall TW, Kim Y-M, Bebbington MWP, Bourissou D, Gabbaï FP. J. Am. Chem. Soc. 2008; 130:10890–10891. [PubMed: 18652460]

30. Caputo CB, Hounjet LJ, Dobrovetsky R, Stephan DW. Science. 2013; 341:1374–1377. [PubMed: 24052304]
31. Bayne JM, Stephan DW. Chem. Soc. Rev. 2016; 45:765–774. [PubMed: 26255595]
32. Studenov AR, Adam MJ, Wilson JS, Ruth TJ. J. Labelled Compd. Radiopharm. 2005; 48:497–500.
33. Ghorab MF, Winfield JM. J. Fluorine Chem. 1990; 49:367–383.
34. Schmutzler R. J. Am. Chem. Soc. 1964; 86:4500–4502.
35. Böttcher T, Shyshkov O, Bremer M, Bassil BS, Röschenthaler G-V. Organometallics. 2012; 31:1278–1280.
36. Ting R, Harwig CW, Lo J, Li Y, Adam MJ, Ruth TJ, Perrin DM. J. Org. Chem. 2008; 73:4662–4670. [PubMed: 18489162]
37. Liu SL, Lin TP, Li D, Leamer L, Shan H, Li ZB, Gabbai FP, Conti PS. Theranostics. 2013; 3:181–189. [PubMed: 23471211]

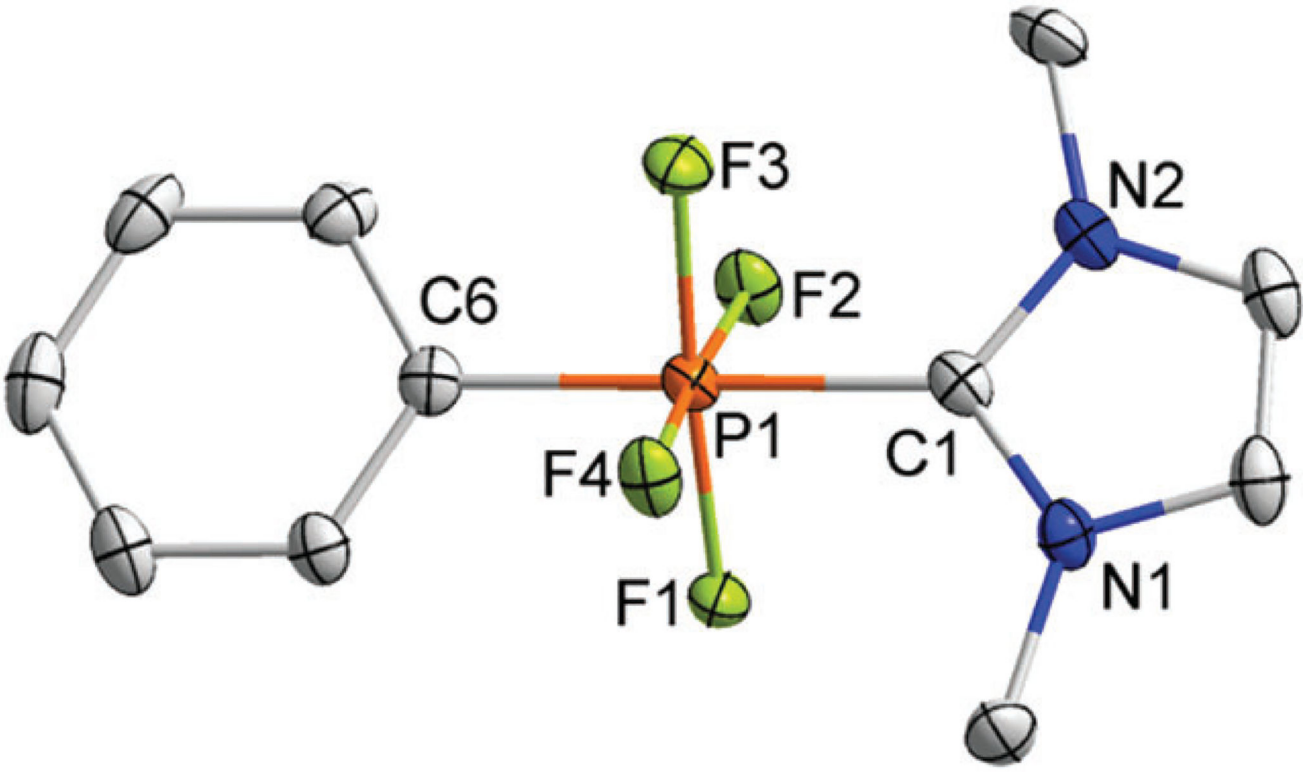

Fig. 1.

ORTEP diagram of **2**. Thermal ellipsoids are shown at the 50% probability level. Hydrogen atoms are omitted for clarity. Selected bond distances (Å) and angles (°): P(1)–C(6) = 1.839(2); P(1)–F(1) = 1.634(1); P(1)–F(2) = 1.642(1); P(1)–F(3) = 1.631(1); P(1)–F(4) = 1.645(1); P(1)–C(1) = 1.898(2); C(1)–P(1)–(C6) = 178.96(6); F(2)–P(1)–F(4) = 175.75(4); C(6)–P(1)–F(1) = 91.76(6).

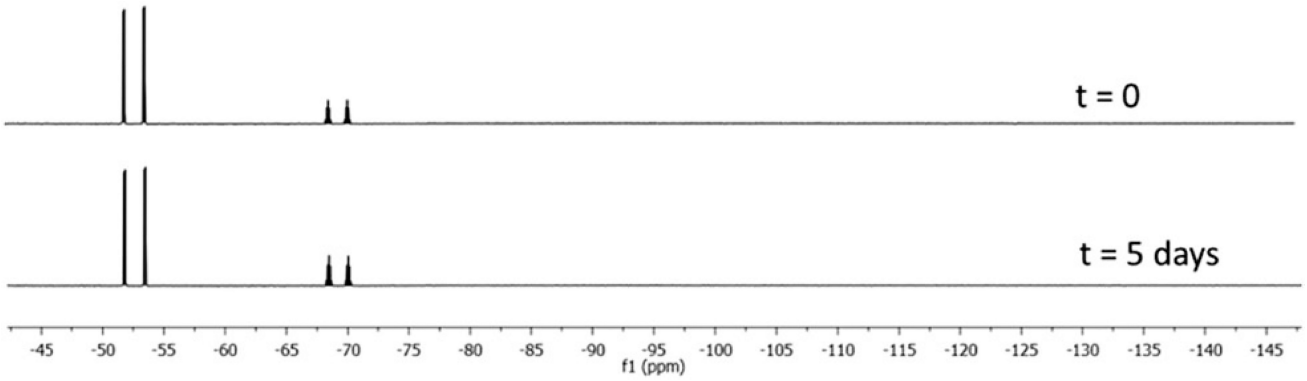

Fig. 2.

^{19}F NMR spectrum of **1** in D_2O–CD_3CN (8/2 vol) phosphate buffer solution at $t = 0$ and $t =$ 5 days.

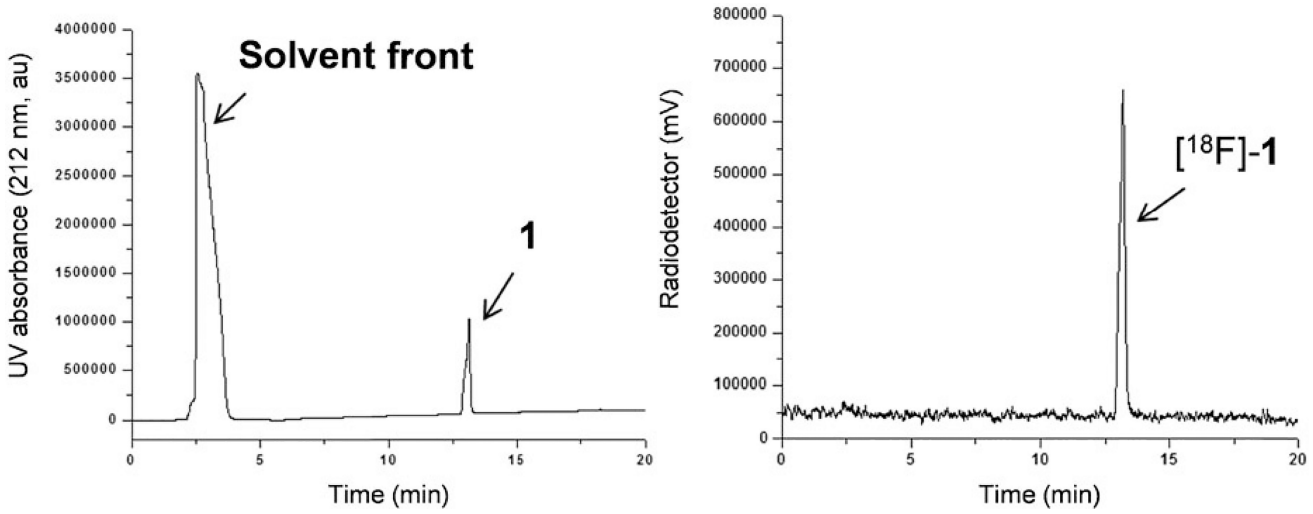

Fig. 3.
Left: UV trace of **1** as the standard reference. Right: Radio-HPLC profile of ^{18}F-[**1**].

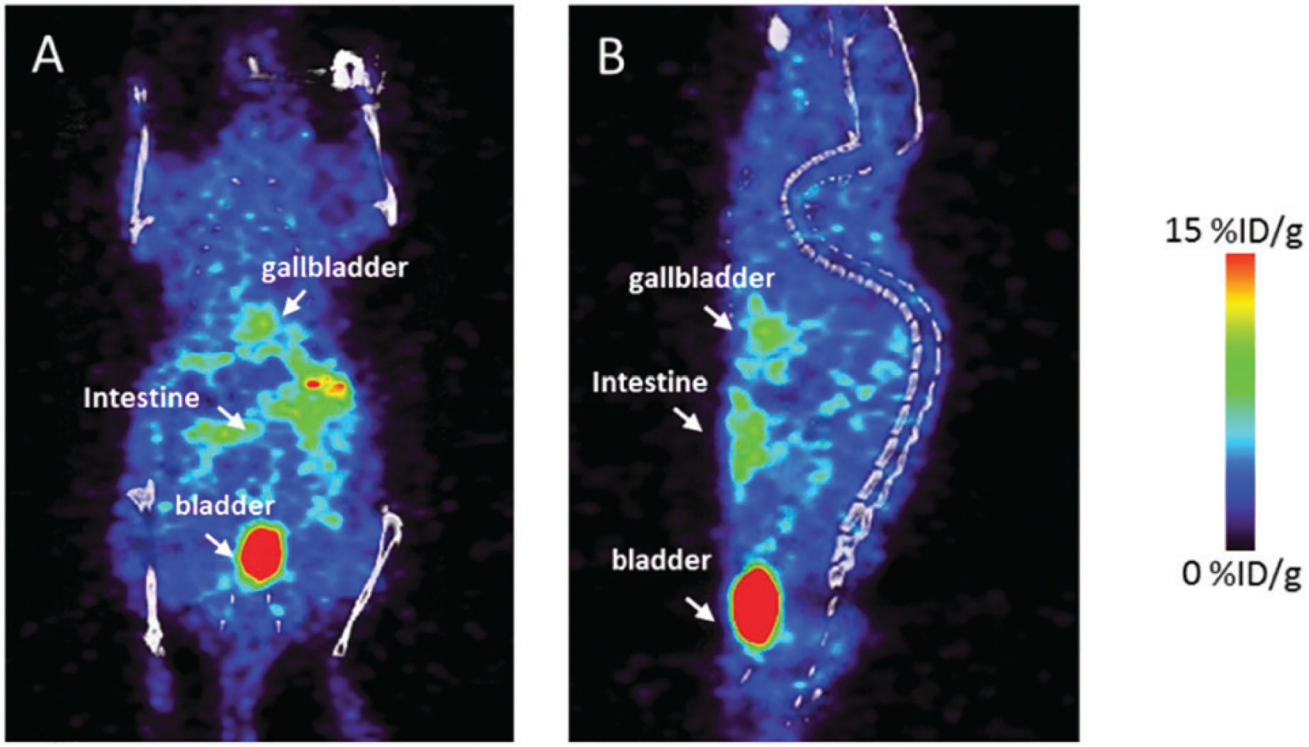

Fig. 4.

Decay-corrected whole-body microPET-CT images of nude mice from a static scan at 3 h after injection of [^{18}F]-**1**. (A) Coronal image and (B) sagittal image.

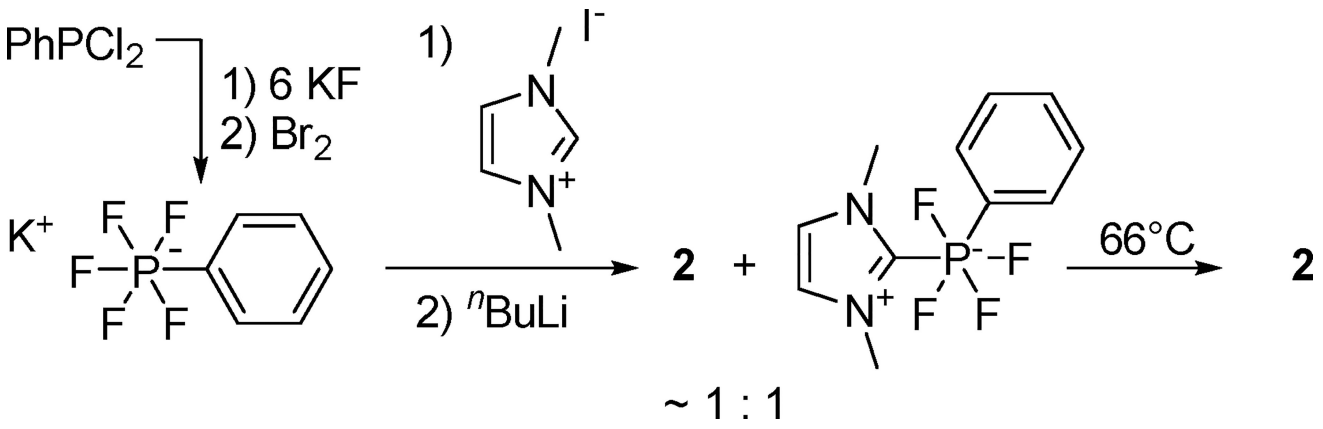

Scheme 1.

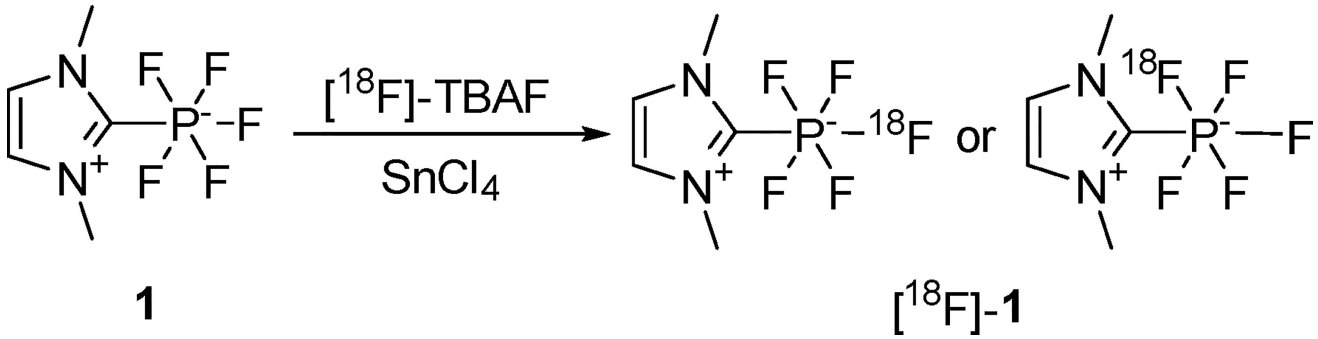

1 **[18F]-1**

Scheme 2.

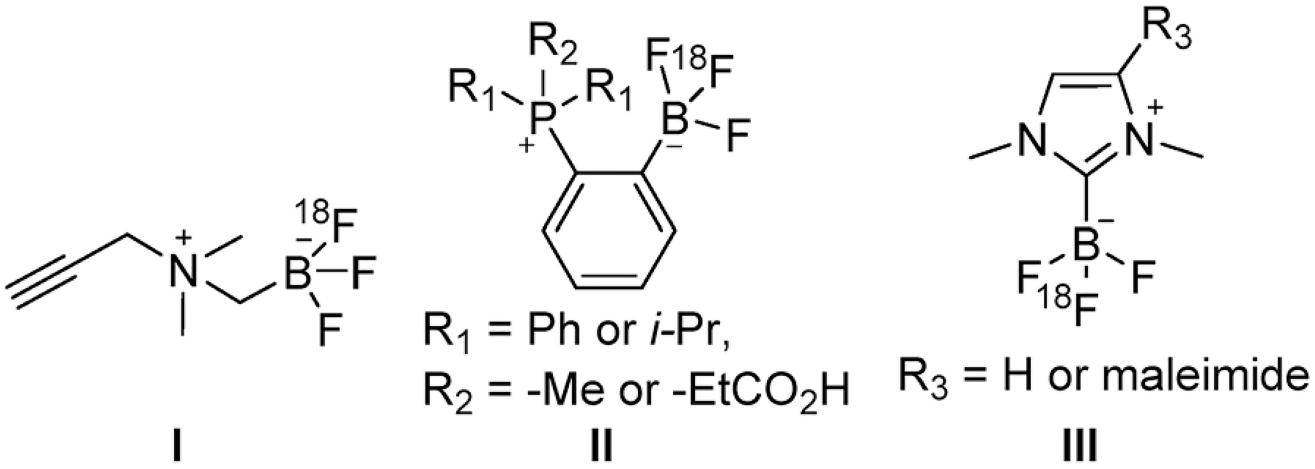

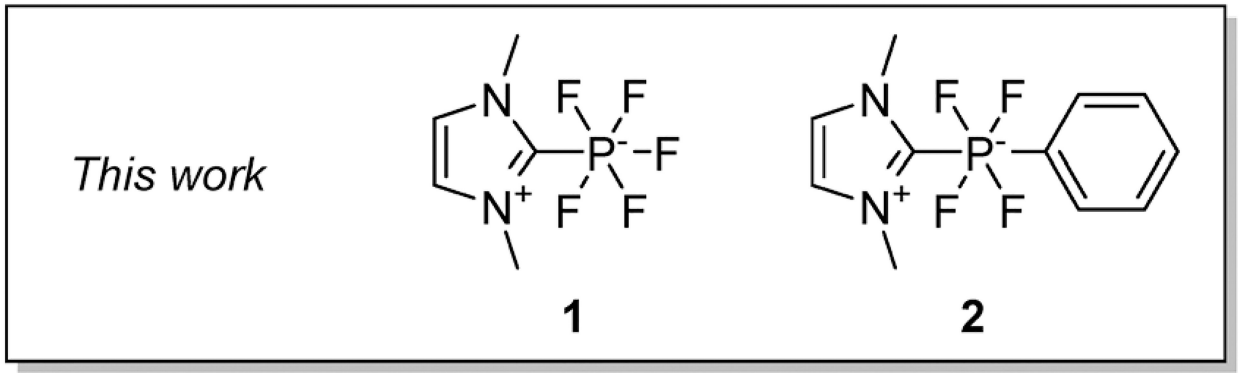

Chart 1.

Table 1

Radiosynthetic results for [^{18}F]-**1**

Entry	[1] (μmol)	$SnCl_4$ (equiv.)	Temp. (°C)	Time (min)	SA[a] (mCi μmol^{-1}) (n = 3)[c]	RCY[b] (%) (n = 3)[c]
1	0.9	5	25	10	No [^{18}F]-**1** observed	
2	0.9	5	60	10	22.6 ± 0.6	4.3 ± 0.3
3	0.9	5	80	10	33.9 ± 1.5	6.6 ± 0.4

[a]Specific activity is determined by dividing the product activity by the amount of the product (based on the integration of UV-HPLC and comparing with the UV chromatogram of the standard).

[b]RCY = activity of the isolated product/starting ^{18}F activity. All yields are decay corrected.

[c]Each experiment was repeated 3 times.